CrossMark

Analysis and field test on reactive capability of photovoltaic power plants based on clusters of inverters

Jingsheng HUANG[1], Meiying LIU[1], Junjun ZHANG[1],
Wei DONG[1], Zhilei CHEN[1]

MPCE

Abstract   With the increasing capacity of photovoltaic (PV) power plants connected to power systems, PV plants are often required to have some reactive power control capabilities to participate in reactive power regulation. Reactive power regulation of grid-connected PV inverters can be achieved using different control strategies. In this paper, the reactive power capability of inverters and the technical requirement of PV plants are analyzed. The reactive power capability of a 30 MW PV plant is evaluated against relevant technical standards using a new testing method proposed in this paper.

1 Introduction

The output of a photovoltaic (PV) power plant is affected by variable insolation, due to atmospheric effects, resulting in volatile and random characteristics [1–4]. When the grid voltage fluctuates, due to variable PV power injection or for other reasons, a PV power plant configured simply to provide active power output cannot provide reactive current to support grid voltage. However, new connection standards require the PV power plant to provide certain reactive current when disturbances are detected at point of interconnection (POI), to help maintain the voltage within the threshold range demanded by technical standards.

Currently, the reactive power sources of PV power plants include static synchronous compensators (STATCOMS) which are static reactive compensation devices, and PV inverters which can provide dynamic reactive power compensation. PV power plants are usually equipped with automatic voltage control (AVC), which can use different reactive power sources in a coordinated way. Reference [5] shows that the AVC system sets the reactive power level according to the bus voltage and total reactive load of both dispatching center and plants. The plant can regulate the POI voltage within normal range through certain strategies. Reference [6] introduces a power decoupling control strategy based on instantaneous reactive power theory, and puts forward the corresponding relation between the power components in the α–β two-phase coordinate system and the compensation current in the three-phase inverter system. It can realize inverter-based reactive power compensation and harmonic current compensation. The active/reactive power control field test and analysis of PV power plants is shown in [7]. But the paper only analyzed the reactive power control curve, carrying out no tests because of the lack of integrated control system.

PV inverters have the ability to receive AVC system instructions and adjust reactive power, as the main reactive power source of PV plant. In this paper, the reactive power output and control capability of clusters of inverters are discussed. After this analysis, a PV power plant without a STATCOM is tested on its reactive power output and

✉ Meiying LIU
  liumeiyin@epri.sgcc.com.cn

  Jingsheng HUANG
  huangjingsheng@erpi.sgcc.com.cn

  Wei DONG
  dongwei@epri.sgcc.com.cn

  Zhilei CHEN
  chenzhilei@epri.sgcc.com.cn

[1] China Electric Power Research Institute, Beijing, China

STATE GRID
STATE GRID ELECTRIC POWER RESEARCH INSTITUTE

Springer

control capability, and the test result is compared with the analysis. Specially, a new method to verify the plant capability to regulate voltage at POI is proposed and used.

2 Analysis on reactive power capability of PV plant

When the inverters are used as a reactive power source, reactive power output of PV power plants depends on the capability of inverters and the internal transmission loss. The loss comes from unit transformers, main transformer and collector lines. An equivalent circuit of a single inverter within the plant connected to grid is shown in Fig. 1. U_{gi} is voltage of inverter output; U_s the voltage of internal busbar; δ_i the phase angle of inverter output; Xi the reactance of transformer and line; P_{Ii} the active power of inverter; Q_{Ii} the reactive power of inverter; S_i the apparent power of inverter; P_i the active power gathered in busbar; and Q_i the active power gathered in busbar.

2.1 Inverter reactive power range

It is well known that the power equation is [8]:

$$P_i = \frac{U_s U_{gi} \sin \delta_i}{X_i} \tag{1}$$

$$Q_i = \frac{U_s(U_{gi} \cos \delta_i - U_s)}{X_i} = \frac{U_s U_{gi} \cos \delta_i}{X_i} - \frac{U_s^2}{X_i} \tag{2}$$

From (1) and (2), it is deduced that

$$P_i^2 + \left(Q_i + \frac{U_s^2}{X_i}\right)^2 = \left(\frac{U_s U_{gi}}{X_i}\right)^2 \tag{3}$$

When $Q_i = 0$:

$$P_i = \sqrt{\left(\frac{U_s U_{gi}}{X_i}\right)^2 - \left(\frac{U_s^2}{X_i}\right)^2} = \frac{U_s}{X_i}\sqrt{U_{gi}^2 - U_s^2} \tag{4}$$

Equation (3) can give the range of reactive power that the inverter can supply to the bus bar:

$$-\sqrt{\left(\frac{U_s U_{gi}}{X_i}\right)^2 - P_i^2} - \frac{U_s^2}{X_i} \leq Q_i \leq \sqrt{\left(\frac{U_s U_{gi}}{X_i}\right)^2 - P_i^2} - \frac{U_s^2}{X_i} \tag{5}$$

Due to the limited apparent power of a PV inverter, the power output range is shown as the shaded region in Fig. 2. Generally, the maximum current is not allowed to exceed 1.1 I_N, where I_N is the nominal maximum current, and
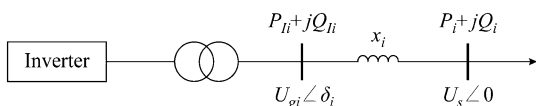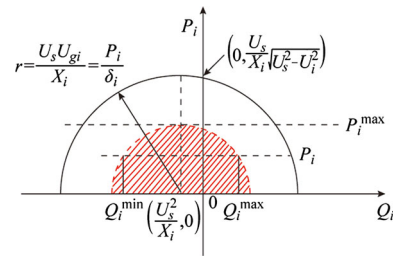

Fig. 1 PV power plant equivalent circuit

Fig. 2 Output characteristic of an inverter

when $P_{Ii} = 1$ p.u., $Q_{Iimax} = 0.46$ p.u; when $P_{Ii} = 0$, $Q_{Iimax} = 1.1$ p.u.

To maintain the active power output of PV power plants, inverters normally operate at rated active power, and therefore the reactive power output range is -0.46 p.u. $\leq Q_{Ii} \leq 0.46$ p.u., which is directly tied to the limiting current of inverters.

2.2 Transformer reactive power loss

The transformer reactive power loss includes the short-circuit loss and the no-load loss [9, 10]. It is defined as:

$$\Delta Q_T = \left[\frac{I_0(\%)}{100} + \frac{U_K(\%)}{100} \times \beta^2\right] S_e \tag{6}$$

$$\Delta Q_K = \frac{U_K(\%)}{100} \times \beta^2 \times S_e \tag{7}$$

where I_0 (%) is no-load current; U_k (%) the short-circuit voltage; β the load factor; S_e the rated capacity; ΔQ_T the total reactive power loss in transformer; and ΔQ_K is the load reactive power loss in transformer.

2.3 Collector lines reactive power loss

The reactive power loss in collector lines consists of line equivalent reactance and equivalent admittance. The latter is proportional to the square of applied voltage and not directly related to the transmission lines, thus not included in the calculations, therefore the line reactive power loss is:

$$\Delta Q_L = 3I^2 \omega L l \tag{8}$$

Therefore, the total reactive power output of PV power plant is:

$$Q = \sum Q_{Ii} - \sum \Delta Q_K - \sum \Delta Q_L \tag{9}$$

3 PV power plant reactive power control on inverters

To control reactive power PV power plants usually use an AVC system consisting of a calculator module and a reactive power distribution module. The calculator module
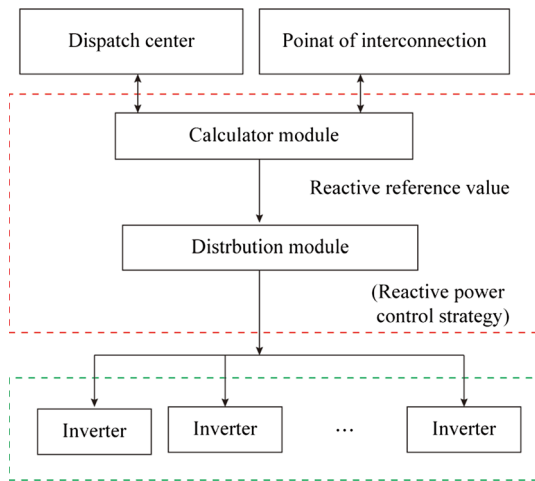
Fig. 3 AVC system data flow

calculates the desired reactive power demand for a PV power plant according to the voltage difference on the low-voltage side of the POI, accounting for the operating constraints of the PV power plant, and finally sets a reasonable value of reactive power. Meanwhile, the calculator module can directly receive reactive power instructions issued from the dispatch center.

The distribution module allocates the reactive power demand value, which is given by the calculator module, to reactive power sources in the PV power plant according to operating status. The flow of data in such an AVC system is shown in Fig. 3.

The PV inverters receive AVC instructions to carry out reactive power regulation as reactive power sources. Grid-connected PV inverters usually adopt power decoupling control, which sets up outer-loop voltage and inner-loop current by converting a stationary coordinate system into a rotating coordinate system [9–12].

Under steady-state conditions, PV inverters can operate in Q_u (voltage control mode), $Q_{\cos\varphi}$ (power factor control mode), and Q_c (reactive power control mode). The model of decoupling control is shown in Fig. 4, and the reference
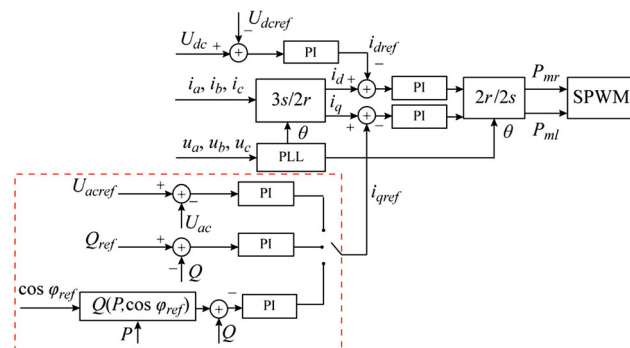

Fig. 4 Inverter decoupling model

I_{qref} (reactive current reference value) is decided according to the operating mode. PV inverters have the ability to receive instruction from AVC system using any operating mode and thereby participate in the grid voltage regulation.

4 Standards and testing procedure

Currently, reactive power regulation of PV power plants is required by domestic and international standards. The German Federal Association of Energy and Water (BDEW) published "Generating Plants Connected to the Medium-voltage Network (Guideline for generating plants' connection to and parallel operation with the medium-voltage network)" [13–15], in which the PV plants are expected to have the ability to regulate the voltage within a certain range. In China, National Standards GB/T 19964-2012 [16] and GB/T 29319-2012 [17], it is clearly stated that the PV plants should participate in voltage regulation according to grid voltage.

The standards require that the reactive power ability of PV plants should be tested and the test items include reactive power output capability, reactive power control capability and control mode.

Reactive power output capability testing is designed to verify the maximum inductive reactive power and capacitive reactive power. Reactive power control capability testing aims to verify the control accuracy and response time when plant receives instruction. Also the plant has to demonstrate its ability to generate reactive power under Q_u, $Q_{\cos\varphi}$ and Q_c modes.

To perform a Q_u (voltage control mode) test, it is necessary to create a voltage disturbance to simulate voltage fluctuation. However, when a PV power plant is online and generating, the grid voltage at the POI stays within narrow limits in most of the time. Moreover, the conventional device used for testing low voltage ride through (LVRT) or grid-disturbance of inverters cannot make enough disturbance because its capacity is far less than that of the PV power plant. To resolve this problem and permit an adequate Q_u (voltage control mode) test, a field testing method is presented which combines transformer tap changing and AVC system adjusting.

In the following section, the reactive power capability of a 30 MW PV power plant is analyzed and field testing is carried out.

5 Field-testing result analysis

The PV power plant under test is located in China. It has 30 units of capacity 1 MW, each with two inverters stepped up through a common transformer to connect to an internal
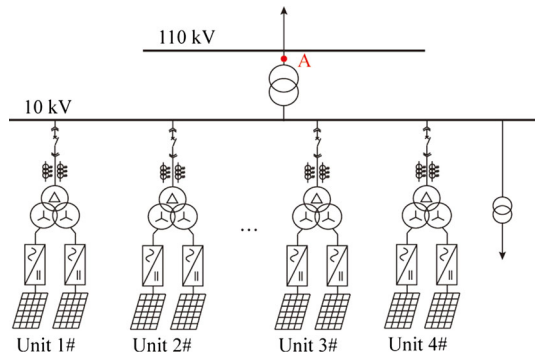
Fig. 5 Single-line diagram of the PV plant under test

10 kV bus bar, and finally stepped up to 110 kV through the main transformer. The PV power plant is connected to grid at 110 kV. During the test, the data recorder is installed at point A on the high-voltage side of the main transformer, as shown in Fig. 5.

5.1 Reactive power output capability

The nominal maximum reactive output of PV inverters is ± 0.55 p.u. (when the power factor equals 0.85). The internal reactive power loss which is calculated according to (6)–(9), is listed in Table 1.

Therefore, when the PV plant generates at full power, the theoretical reactive power output is:

$$Q = \sum Q_{Ii} - \sum \Delta Q_K - \sum \Delta Q_L = 6.197 \text{ MVar} \quad (10)$$

$$\frac{Q}{Q_N} = 0.2 \text{ p.u.} \quad (11)$$

During the test period, the maximum irradiation is 533 W/m^2 while the output active power of PV power plant is $P_0 = 16$ MW. The reactive power output capability is tested at every 10 % step of P_0 and the result is shown in Fig. 6. Q_C is the capacitive reactive power of PV power plant, and Q_L is the inductive reactive power of PV power plant.

It can be seen from Fig. 6 that the maximum Q_C of plant reaches almost 0.48 p.u. when the irradiation is low, and the maximum Q_L of plant reaches almost 0.53 p.u. The reactive power output is slightly less than calculated because of the loss, nevertheless, the output capability meets the standards requirements.

Table 1 Reactive power loss

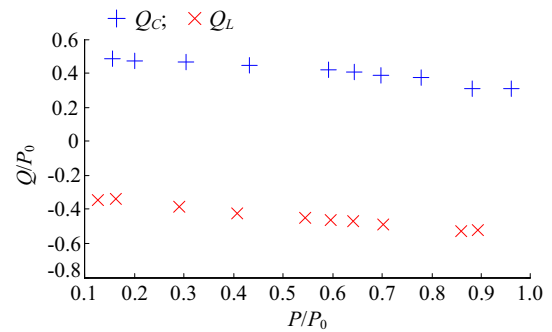| Main transformer (Mvar)	Unit transformer (Mvar)	Collecting line (Mvar)
3.932	2.136	0.129

Fig. 6 Reactive output capability

5.2 Reactive power control capability

The reactive power control capability is carried out when the active power is about 50 % P_0. The plant is set to follow the reactive output curve 0-Q_C-Q_L-0 and the result is shown in Fig. 7. The reactive power step response times are shown in Table 2, and it can be seen that the plant has the reactive power control capability, and the response time is lesser than 10 s. The results meet the requirement in GB/T 19964-2012 and GB/T 29321-2012.

5.3 Reactive power control mode

In this section, tests are reported for Q_u mode (voltage control) and $Q_{\cos\varphi}$ mode (power factor control) respectively.

1) Q_u mode (voltage control)

Before the test, PV power plant is set to operate under Q_u mode (voltage control). The reference voltage is set to
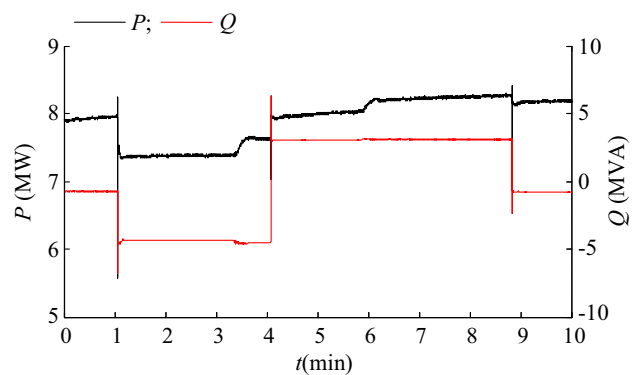

Fig. 7 Reactive control capability

Table 2 Response time for reactive power control

Step	0-Q_C	Q_C-Q_L	Q_L-0
Time (s)	0.3	0.4	0.4

1.0 U_n and the threshold to ± 2 % by the AVC system, which means the system monitors voltage at the POI and will regulate voltage exceeding the range of 0.98–1.02 U_n by adjusting inverters' reactive outputs. The main transformer is provided with an on-load tap changer, which has a short-circuit impedance of 10.8 %. The transformer has ± 10 adjustment range with 1.25 % increments.

During the test, the voltage is adjusted to exceed the limits using the on-load tap changer, and the response of the inverters is recorded and analyzed.

As shown in Fig. 8, by adjusting the on-load tap changer, the bus voltage is raised over the threshold value. At this time the plant calculates and dispatches the reactive power to inverters, to stabilize voltage in the normal range.

By the detailed view in Fig. 9, it can be seen that the reactive current changed after the voltage rise over the threshold value in several seconds. The reactive power and response time is calculate and shown in Table 3. The response time is measured from the voltage changing over preset value.
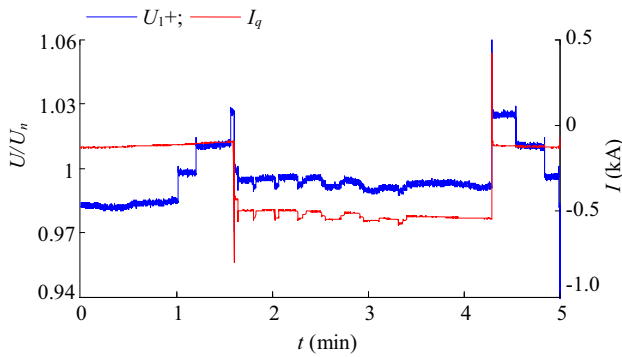

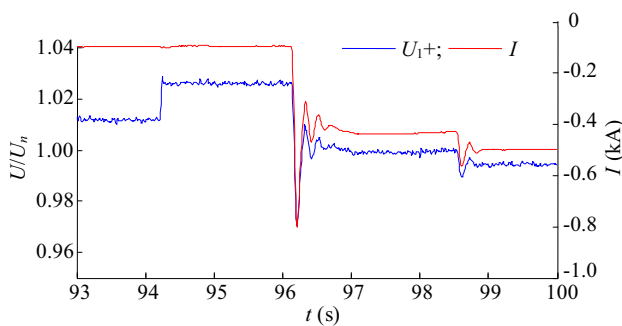**Fig. 8** Voltage and reactive current (over 5 min)

Fig. 9 Voltage and reactive current (over 7 s)

Table 3 Q_u mode test result

Range	Before	After
U (p.u.)	1.028	1.00
Reactive power (Mvar)	−0.1	−0.5
Response time (ms)	1920	

2) $Q_{\cos\varphi}$ mode (power factor control)

When plants operate under $Q_{\cos\varphi}$ mode, the system keep monitoring the power factor at the POI, and calculates and dispatches instructions to the inverters, so that they generate reactive power to make the power factor equal to a requested value.

During the test, the plant firstly was asked to adjust $\cos\varphi$ from 1.0 to 0.95, then 5 min later to adjust $\cos\varphi$ from 0.95 to 1, and finally after another 5 min to adjust the power factor from 1 to −0.95.

The bus voltage, reactive power, power factor at the low voltage side (10 kV) of the first test is shown in Fig. 10.

The figure shows that the reactive power increases after the AVC system sent out the power factor set value. The power factor changed from 1 to 0.965 after a delay of 1.6 s.

Then the power factor is set from 0.965 to 1, and the result is shown in Fig. 11. The power factor changed from 0.965 to 0.999 after a delay of 1.2 s.

After that, the power factor is set from 1 to −0.95 and the result is shown in Fig. 12. The figure shows that it takes 1.2 s to make power factor change from 1 to −0.968.

The accuracy of unit power factor is very good, but the accuracy of plant is poor, which could be caused by several reasons: ① it could be caused by reactive power losses which may be larger than expected in Table 1; ② it is assumed that the sum of inverters' output is less than multiplication of single inverter because of the deviation of phase angle. And further experiments are planned to be performed to reveal the real reason.

Obviously, the power factor control accuracy needs to be improved, but the field test proves that the plant has the ability to work under Q_u mode (voltage control) and $Q_{\cos\varphi}$ mode (power factor control).
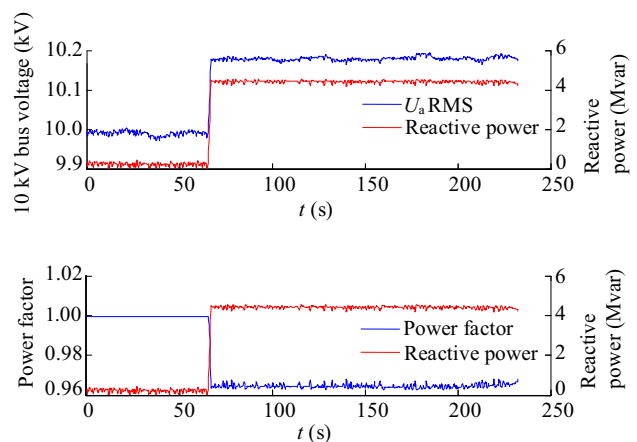

Fig. 10 10 kV voltage, reactive power and power factor when AVC requests power factor from 1 to 0.95
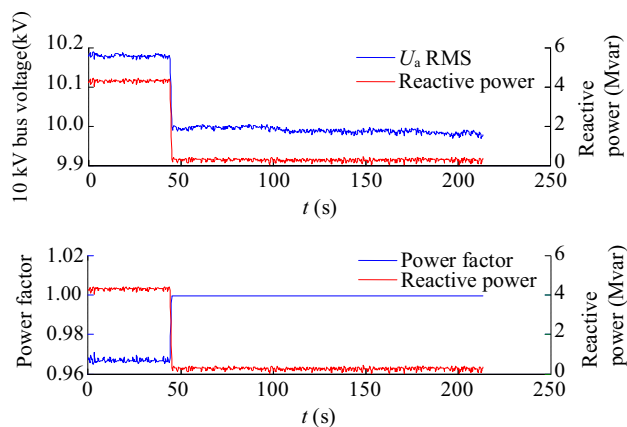
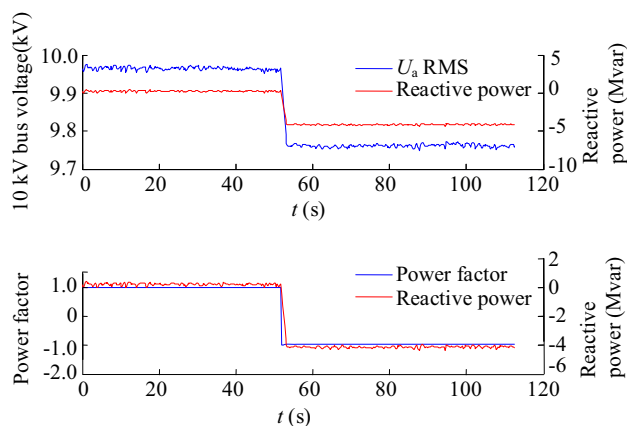**Fig. 11** 10 kV volage, reactive power and power factor when AVC requests power factor from 0.95 to 1

Fig. 12 10 kV voltage, reactive power and power factor when AVC requests power factor from 1 to −0.95

6 Conclusion

In this paper, reactive power output capacity and control capability of PV plants, using inverters without other compensating device, are theoretically analyzed. The maximum capacity and inductive reactive power control are tested using a 30 MW PV power plant and compared with theoretical value. Voltage control and power factor control operating modes are demonstrated. A new testing method is proposed which combines the AVC system and an on-load tap changer to make voltage disturbances to verify voltage control mode.

References

[1] Yaghoobi J, Mithulananthan N, Saha TK (2014) Effect of PV power injection in unbalanced distribution systems. In: Proceedings of the 2014 Australasian universities power engineering conference (AUPEC'14), Perth, WA, USA, 28 Sept–1 Oct 2014, 6 pp

[2] Dong W, Huang JS, Liu MY (2013) An optimization method of harmonic analysis in IEC framework. In: Proceedings of the 2nd IET renewable power generation conference (RPG'13), Beijing, China, 9–11 Sept 2013, 4 pp

[3] Reno MJ, Coogan K, Grijalva S et al (2014) PV interconnection risk analysis through distribution system impact signatures and feeder zones. In: Proceedings of the 2014 IEEE PES general meeting, National Harbor, MD, USA, 27–31 Jul 2014, 5 pp

[4] Srisaen N, Sangswang A (2006) Effects of PV grid-connected system location on a distribution system. In: Proceedings of the IEEE Asia Pacific conference on circuits and systems (APC-CAS'06), Singapore, 4–7 Dec 2006, pp 852–855

[5] Wei SG, Liu S (2013) Application of AGC/AVC in photovoltaic power station. Jiangsu Electr Eng 32(2):35–42 (in Chinese)

[6] Zhang GR, Qi GH, Su JH et al (2010) Relation between current components and *p–q* power components in three-phase system. Power Syst Technol 34(7):64–69 (in Chinese)

[7] Dong KS, Li HT, Li Z et al (2013) Field testing and analysis of control capability of active/reactive power for photovoltaic power station. Power Syst Clean Energ 29(11):82–85 (in Chinese)

[8] Chen B (2012) Research on voltage and VAR coordination control technologies of large-scale grid-connected photovoltaic power station. Master Thesis, State Grid Electric Power Research Institute, Nanjing, China (in Chinese)

[9] Xing ZX, Dong HN, Cheng XK et al (2012) Research the example of reactive power based on DIgSILENT when wind farm integrated into the power system. Electr Eng 8:10–13 (in Chinese)

[10] AgüeroA JL, Arnera PL, Lastra REB et al (2006) Synchronous compensators: models verified by tests of automatic voltage regulator, reactive power control, and voltage joint control. IEEE Trans Power Syst 21(4):1798–1807

[11] Tang YH, Xu L, Fan H et al (2013) Real-time simulation based closed-loop detection for AVC system of regional power grid. Power Syst Technol 37(9):2515–2520 (in Chinese)

[12] Sun JW, Wang ZX, Xia YJ et al (2014) Study on distributed reactive power and voltage automatic control in regional smart grid. Power Syst Protect Control 42(13):112–116 (in Chinese)

[13] Wang SY, Zhu LZ, Chen N et al (2009) A reactive power control strategy for wind farm based on hierarchical layered principle. Autom Electr Power Syst 33(13):83–88 (in Chinese)

[14] Technical Guideline (2008) Generating plants connected to the medium-voltage network. BDEW (Bundesverband der Energie und Wasser), Berlin, Germany

[15] Liu MY, Huang JS, Zhang JJ et al (2014) Model validation and error analysis of photovoltaic grid-connected inverter based on BDEW standard. Autom Electr Power Syst 38(13):196–201. doi:10.7500/AEPS20130922004 (in Chinese)

[16] VDE-AR-N 4105 (2011) Generators connected to the low-voltage distribution network—Technical requirements for the connection to and parallel operation with low-voltage distribution networks

[17] GB/T 19964–2012 (2012) Technical requirements for connecting photovoltaic power station to power system (in Chinese)

Jingsheng HUANG received the B.Sc, M.Sc. degrees from Southeast University, China, in 2004, and 2007 respectively. He is now a Senior Engineer in New Energy Department, China Electric Power Research Institute. His research interests include testing and analysis of PV power plant, power quality, and PV yield analysis.

Meiying LIU received the M.sc. degrees from Harbin Institute Technology, China, in 2010. She now works for China Electric Power Research Institute. Her research interests include testing and analysis of PV plant, PV power grid performance evaluation.

Junjun ZHANG is a Senior Engineer in New Energy Department, China Electric Power Research Institute. He received the B.Sc, M.Sc. degrees from Hefei University of Technology, China, in 2004 and 2007 respectively. His research interests include testing technology of PV modules, balance components and system, testing and evaluation technology for grid-connected renewable energy, standardization on PV testing.

Wei DONG received the B.Sc, M.Sc. degrees from Hefei University of Technology, China, in 2008, and 2012 respectively. He now works for the China Electric Power Research Institute. His research interests include PV grid test technology, PV power grid performance evaluation.

Zhilei CHEN received the M.Sc degrees from Northwestern Polytechnical University, China, in 2004. His research interests include testing technology of PV modules, balance components and system, standardization of test technology for grid-connected renewable energy.